Optimal Propeller Orientations for a Fully-actuated UAV with an Off-center Payload

Ahmed Ali*, Fiorella Romano#, Barbara Bazzana*, Chiara Gabellieri*, Fabio Ruggiero#, Antonio Franchi*,†

***Abstract*— Physical inspection tasks often require a sensor to be mounted on an end-effector, causing the vehicle's center of mass to shift away from its geometric center. In this extended abstract, we investigate the effect of such an off-center payload on the design of a fixedly tilted fully-actuated octarotor. In particular, results show how the CoM shift changes the optimal rotor orientations. The proposed analysis also shows that, irrespective of the shift, the optimal direction of each propeller lies on the plane perpendicular to the line between that propeller center and the geometric center of the robot chassis.**

I. INTRODUCTION

Due to their versatility, simplicity, and suitability for a wide range of applications, multirotor aerial vehicles (MRAVs) have been extensively studied in recent years [1]. Traditional multirotor designs, such as quadrotor or hexarotors, typically feature fixed, coplanar propellers with parallel angular velocities. These configurations are underactuated, meaning that not all six degrees of freedom (DoFs) can be independently controlled [2]. As a consequence, horizontal motion can only be achieved by tilting the vehicle, which limits maneuverability and prevents full decoupling of position and attitude. This limitation has motivated the development of new MRAV designs that explore alternative numbers, positions, and orientations of propellers to provide enhanced actuation capabilities. Among these, omnidirectional and morphing multirotors have attracted significant attention. Omnidirectional platforms can sustain their weight and generate forces in any direction, enabling independent control of position and orientation [3]. Various approaches exist to achieve decoupled position and attitude control [4]. A design that aims at maximizing the wrench space of the vehicle is proposed in Brescianini *et al.* [5] where the vehicle is equipped with fixed bi-directional propellers placed at the vertexes of a cubic frame. Morphing designs with actively tilting propellers are another technique employed to achieve omnidirectional wrench generation by dynamically change the orientation of the propeller such that the desired wrench is realized [6]–[9]. In Franchi [10], the optimal design problem is studied for a large class of multirotor designs. The mathematical modeling of these designs is typically carried out under the assumption that the CoM of the vehicle always coincides with its geometric center.

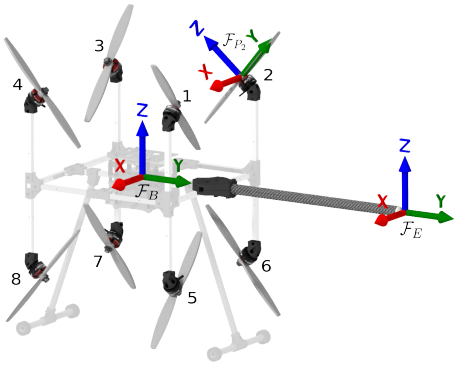

Fig. 1: Schematic representation of the considered fully actuated octarotor.

In the literature, a shifted CoM is often treated as an external disturbance rather than being incorporated into the system model. For example, in Bodie *et al.* [11], the effect of the CoM shift is compensated through a wrench estimator combined with an impedance controller, without explicitly updating either the dynamics or the control-allocation model. As a consequence, the reported simulations and experiments exhibit a residual steady-state torque offset. Another strategy, proposed in Fresk *et al.* [12], estimates the center of gravity online via an EKF and update the control-allocation matrix accordingly, enabling compensation of both abrupt and gradual payload-induced shifts. However, their approach still does not revise the dynamic parameters of the robot, such as the inertia matrix, to account for the displaced CoM.

Related work on omnidirectional aerial vehicles with unidirectional thrusters has also highlighted the importance of conditioning of the allocation matrix. In particular, inspired by Tognon and Franchi [13], we here use the condition number of the allocation matrix as a design metric.

In this work, we consider an 8-propeller Omnirotor platform [14], whose rotors are placed at orientations defined

The first two authors can both be considered as the first author. * Robotics and Mechatronics Department, Electrical Engineering, Mathematics, and Computer Science (EEMCS) Faculty, University of Twente, 7500 AE Enschede, The Netherlands. ahmed.ali@utwente.nl, c.gabellieri@utwente.nl, schol@r-franchi.eu

PRISMA Lab, Department of Electrical Engineering and Information Technology, University of Naples Federico II, 80125 Naples, Italy fabio.ruggiero@unina.it

†Department of Computer, Control and Management Engineering, Sapienza University of Rome, 00185 Rome, Italy. schol@r-franchi.eu

This work was partially funded by the Horizon Europe research agreement no. 101120732 (AUTOASSESS) and NWO OTP AVIATOR.

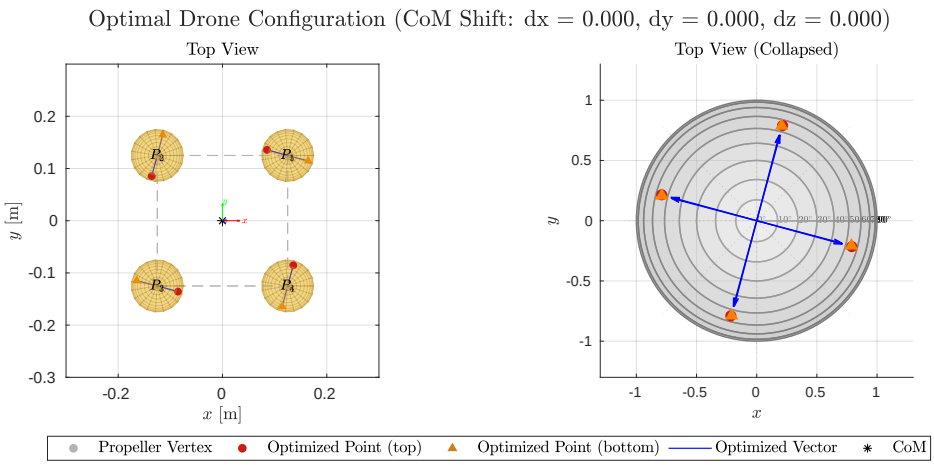

Fig. 2: Optimal orientations for $y_d = 0$. Left: top-view of the octarotor; right: aggregated view of all propeller disks superimposed.

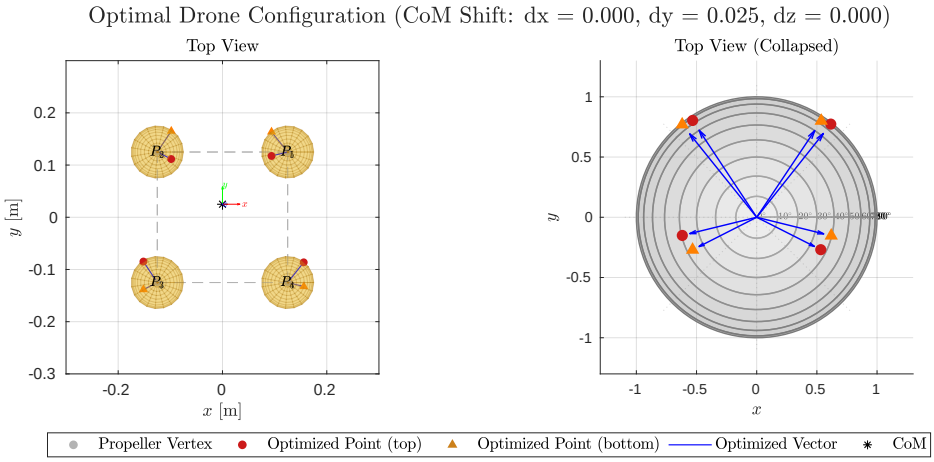

Fig. 3: Optimal orientations with CoM shift $y_d = 0.25L$. Left: top-view; right: aggregated view of all propeller disks superimposed.

by two independent rotations. Owing, for example, to an NDT sensor mounted on the end-effector, the vehicle center of mass does not coincide with its geometric center. We investigate how the optimal propeller directions vary as the CoM shifts. Our results show that the optimal directions of the propellers depend on the CoM shift. Nonetheless, all the optimal directions lie on the plane perpendicular to the vector connecting the geometric center of the propeller's positions to the propeller location.

We first present the vehicle dynamic model, followed by the optimization problem. We then present simulation results illustrating the effect of the CoM shift on the optimal design.

II. Dynamic Model

We consider the fully-actuated octarotor with positions of the propellers lying on a cube as in [5], [14]. The CoM of the robot is considered shifted from the propellers' geometric center due to the presence, e.g., of a rigid end effector. A schematic representation of the considered system is in Fig. 1 Let F_W be the inertial frame, F_B a frame fixed to the vehicle and centered at the geometric center of the propeller's positions, and $F_{B_{\text{CoM}}}$ another vehicle-fixed frame centered at the shifted total center of mass (CoM), defined as $O_{B_{\text{CoM}}}$. $O_{B_{\text{CoM}}}$ position in F_B is $\mathbf{d} = (0, y_d, 0)$. Denote by $\mathbf{p} \in \mathbb{R}^3$ the position of $O_{B_{\text{CoM}}}$ in F_W, by $\boldsymbol{\omega}_{B_{\text{CoM}}} \in \mathbb{R}^3$ the body angular velocity expressed in $F_{B_{\text{CoM}}}$.

Let the control input vector be

$$\mathbf{u} = [\bar{w}_1|\bar{w}_1| \ \cdots \ \bar{w}_8|\bar{w}_8|]^T := [u_1 \ \cdots \ u_8]^T \in \mathbb{R}^8, \quad (1)$$

where $\bar{w}_i$ is the angular speed of propeller i. For each propeller, let $\mathbf{n}_i$ its thrust direction expressed in $F_{B_{\text{CoM}}}$, and let its position relative to the shifted CoM be

$$\mathbf{p}_i^{B_{\text{CoM}}} = L\mathbf{s}_i - \mathbf{d}, \qquad i = 1, \dots, 8, \quad (2)$$

with $\mathbf{s}_i \in \{-1, +1\}^3$ denoting the cube-vertex sign pattern and $\mathbf{d}$ the CoM shift. L is the cube half-side length.

The total actuator wrench at $F_{B_{\text{CoM}}}$ is written as

$$\mathbf{w} = \begin{bmatrix} \mathbf{f} \\ \boldsymbol{\tau} \end{bmatrix} = \mathbf{A}\mathbf{u}, \quad (3)$$

with allocation matrix

$$\mathbf{A} = \begin{bmatrix} \mathbf{N} \\ \mathbf{M} \end{bmatrix} \in \mathbb{R}^{6\times 8}, \quad (4)$$

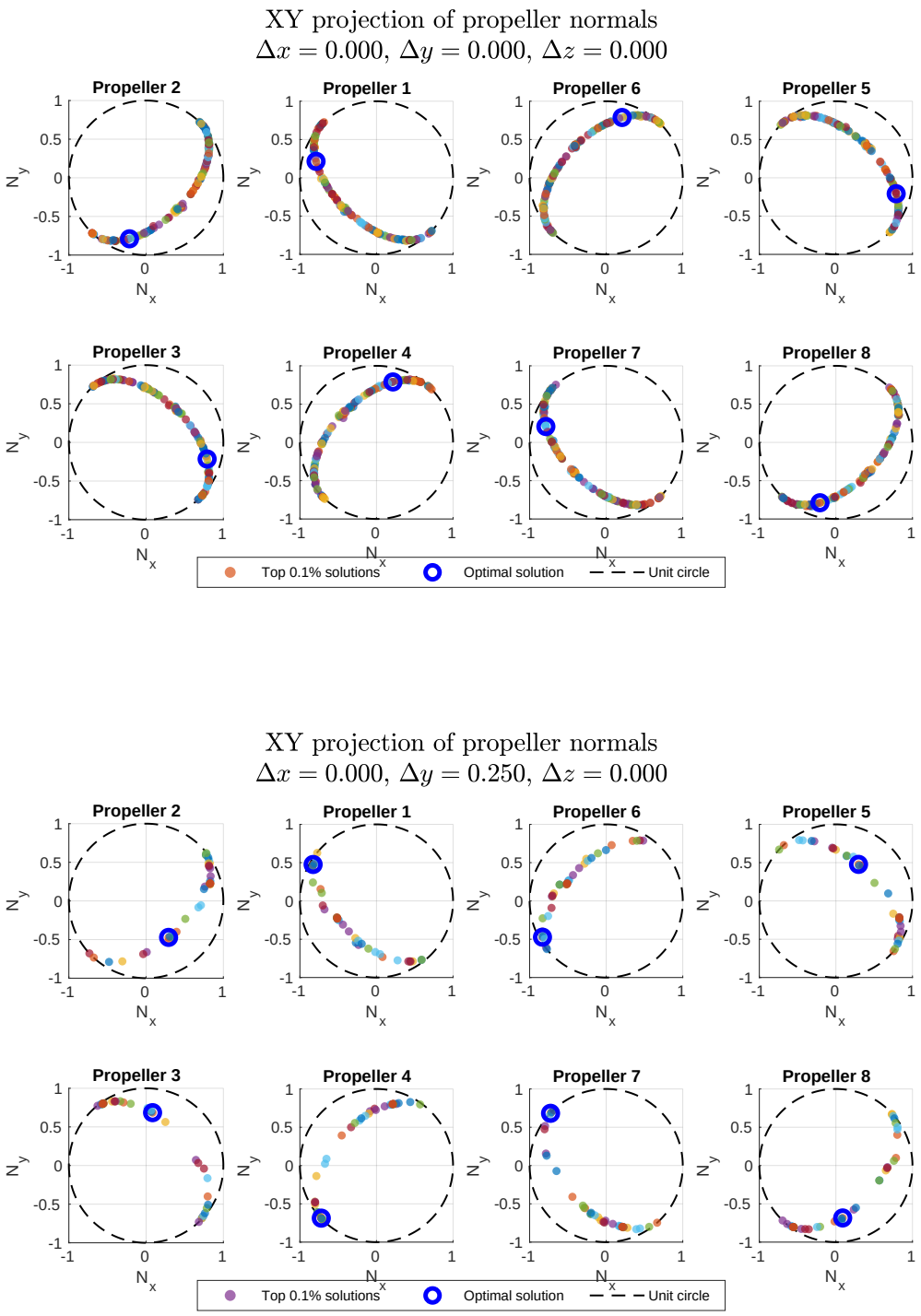

Fig. 4: Projection on the XY plane of the 0.1% near-optimal solutions. Each color uniquely identifies a single solution from the multi-start optimization. Top: without CoM shift; bottom: $y_d = 0.25L$.

$\mathbf{N} = \begin{bmatrix} k_f \mathbf{n}_1 & \cdots & k_f \mathbf{n}_8 \end{bmatrix} \in \mathbb{R}^{3\times 8}$, and

$$\mathbf{M} = \begin{bmatrix} [\mathbf{p}_1^{B_{\text{CoM}}}]_\times k_f \mathbf{n}_1 & \cdots & [\mathbf{p}_8^{B_{\text{CoM}}}]_\times k_f \mathbf{n}_8 \end{bmatrix}.$$

Here, k_f is the thrust coefficient and $[\cdot]_\times$ denotes the skew-symmetric matrix such that $[\mathbf{a}]_\times \mathbf{b} = \mathbf{a} \times \mathbf{b}$. The drag moment contribution has been omitted, assuming its contribution is negligible compared to the thrust-induced torque, similarly to what is done in the state of the art [5], [10]. The complete

Newton-Euler dynamics of the platform are therefore

$$\begin{bmatrix} m\ddot{\mathbf{p}} \\ I_{B_{\mathrm{CoM}}}\dot{\boldsymbol{\omega}}_{B_{\mathrm{CoM}}} \end{bmatrix} = \underbrace{\begin{bmatrix} -m\mathbf{g} \\ -\boldsymbol{\omega}_{B_{\mathrm{CoM}}} \times (I_{B_{\mathrm{CoM}}}\boldsymbol{\omega}_{B_{\mathrm{CoM}}}) \end{bmatrix}}_{\mathbf{f}} + \mathbf{A}\mathbf{u} \quad (5)$$

with $\mathbf{g} = [0 \ 0 \ -g]^T$ the gravity vector, m the mass of the robot, and $I_{B_{\mathrm{CoM}}}$ the rotational inertia. This formulation explicitly captures the CoM shift both in the inertia tensor $I_{B_{\mathrm{CoM}}}$ and in the allocation matrix $\mathbf{A}$ through the shifted positions $\mathbf{p}_i^{B_{\mathrm{CoM}}}$.

III. Design Optimization Problem

The positions of the propellers on the robot's chassis are considered fixed, given parameters. The design objective is to select the propeller orientations so that the resulting allocation matrix remains as well-conditioned as possible under the shifted CoM while preserving full omnidirectional wrench generation. To this end, we optimize the rotor directions $\mathbf{n}_i$, $i = 1, \ldots, 8$, by minimizing the following cost function, where $K > 0$ is a scalar weighting factor

$$\min_{\mathbf{n}_1,\ldots,\mathbf{n}_8} \quad -\sigma_{\min}(\mathbf{A}) + K\frac{\sigma_{\max}(\mathbf{A})}{\sigma_{\min}(\mathbf{A})}, \quad (6)$$

constrained by $\|\mathbf{n}_i\| = 1$. Eq. (6) simultaneously maximizes the minimum singular value of $\mathbf{A}$ and penalizes a large condition number. The problem is nonconvex and solved using a multistart nonlinear procedure. The best local solution is retained as the optimized rotor configuration for the considered shift y_d, which appears in the cost function through matrix $\mathbf{A}$.

IV. Simulation Results

To solve the optimization, a total of 700 initial guesses for the propeller orientations were generated by uniformly sampling points on the upper unit hemisphere.

In Fig. 2, the optimal propeller directions are represented for the case where the CoM and the propeller geometric center coincides. Conversely, Fig. 3 shows the optimal propeller orientations for a shift $y_d = 0.25L$. From this and other tests omitted for the sake of space and carried out for $y_d \in \{0.5L, L, 1.5L, 2L\}$, it emerges that the optimal propeller orientations change with the CoM shift.

Moreover, we observed from numerical results that despite the optimal orientations changing with the CoM shift, they lie on the same plane, orthogonal to the line connecting the propeller center with the center of the cube. Notably, the definition of such a plane does not depend on the shift of the CoM. As an example, in Fig. 4, we report the 0.1% near-optimal solutions with $y_d = 0$ and with $y_d = 0.25L$. The solutions with the CoM shift are less uniformly distributed than in the case with $y_d = 0$. Nevertheless, they fit a curve corresponding to the intersection between the hemisphere spanning the possible propeller orientations and the plane orthogonal to the line connecting each propeller with the center of the cube.

V. Conclusions

The abstract studies the optimal design of a fully actuated octarotor. We have shown the dependency of the optimal solutions on the CoM shift for the considered cost function. In the future, different cost functions will be considered, as well as the effect of the propeller drag moment, and analytical results will be derived.

References

[1] M. Sabour, P. Jafary, and S. Nematiyan, "Applications and classifications of unmanned aerial vehicles: A literature review with focus on multi-rotors," *The Aeronautical Journal*, vol. 127, no. 1309, pp. 466–490, 2023.

[2] R. Mahony, V. Kumar, and P. Corke, "Multirotor aerial vehicles: Modeling, estimation, and control of quadrotor," *IEEE Robotics & Automation Magazine*, vol. 19, no. 3, pp. 20–32, 2012.

[3] M. Hamandi, Q. Sable, M. Tognon, and A. Franchi, "Understanding the omnidirectional capability of a generic multi-rotor aerial vehicle," in *2021 Aerial Robotic Systems Physically Interacting with the Environment (AIRPHARO)*, 2021, pp. 1–6.

[4] R. Rashad, J. Goerres, R. Aarts, J. B. C. Engelen, and S. Stramigioli, "Fully actuated multirotor uavs: A literature review," *IEEE Robotics & Automation Magazine*, vol. 27, no. 3, pp. 97–107, 2020.

[5] D. Brescianini and R. D'Andrea, "Design, modeling and control of an omni-directional aerial vehicle," in *2016 IEEE International Conference on Robotics and Automation (ICRA)*, 2016, pp. 3261–3266.

[6] Y. Aboudorra, C. Gabellieri, R. Brantjes, Q. Sablé, and A. Franchi, "Modelling, analysis, and control of omnimorph: an omnidirectional morphing multi-rotor uav," *Journal of Intelligent & Robotic Systems*, vol. 110, no. 1, p. 21, 2024.

[7] A. Oosedo, S. Abiko, S. Narasaki, A. Kuno, A. Konno, and M. Uchiyama, "Flight control systems of a quad tilt rotor unmanned aerial vehicle for a large attitude change," in *2015 IEEE International Conference on Robotics and Automation (ICRA)*, 2015, pp. 2326–2331.

[8] M. Zhao, T. Anzai, F. Shi, X. Chen, K. Okada, and M. Inaba, "Design, modeling, and control of an aerial robot dragon: A dual-rotor-embedded multilink robot with the ability of multi-degree-of-freedom aerial transformation," *IEEE Robotics and Automation Letters*, vol. 3, no. 2, pp. 1176–1183, 2018.

[9] M. Kamel, S. Verling, O. Elkhatib, C. Sprecher, P. Wulkop, Z. Taylor, R. Siegwart, and I. Gilitschenski, "The voliro omniorientational hexacopter: An agile and maneuverable tiltable-rotor aerial vehicle," *IEEE Robotics & Automation Magazine*, vol. 25, no. 4, pp. 34–44, 2018.

[10] A. Franchi, "The n-5 scaling law: Topological dimensionality reduction in the optimal design of fully-actuated multirotors," *arXiv preprint arXiv:2512.23619*, 2025.

[11] K. Bodie, M. Brunner, M. Pantic, S. Walser, P. Pfändler, U. Angst, R. Siegwart, and J. Nieto, "An omnidirectional aerial manipulation platform for contact-based inspection," *arXiv preprint arXiv:1905.03502*, 2019.

[12] E. Fresk, D. Wuthier, and G. Nikolakopoulos, "Generalized center of gravity compensation for multirotors with application to aerial manipulation," in *2017 IEEE/RSJ International Conference on Intelligent Robots and Systems (IROS)*, 2017, pp. 4424–4429.

[13] M. Tognon and A. Franchi, "Omnidirectional aerial vehicles with unidirectional thrusters: Theory, optimal design, and control," *IEEE Robotics and Automation Letters*, vol. 3, no. 3, pp. 2277–2282, 2018.

[14] R. Veenstra, A. Ali, C. Gabellieri, and A. Franchi, "6d physical interaction with an omnidirectional aerial robot," *Drones*, vol. 10, no. 2, 2026. [Online]. Available: https://www.mdpi.com/2504-446X/10/2/129